POLISH MARITIME RESEARCH 2(78) 2013 Vol 20; pp. 3-12
10.2478/pomr-2013-0011

Comparative analysis of the theoretical models of ideal propulsor, ideal fluid brake, ideal screw propeller and ideal axial wind turbine

Tadeusz Koronowicz, Prof.
The Szewalski Institute of Fluid Flow Machinery, Gdansk, Poland
Jan A. Szantyr, Prof.
Gdansk University of Technology, Poland

ABSTRACT

The article presents a detailed discussion of the theoretical models of four different fluid dynamic devices: an ideal propulsor, an ideal fluid brake, an ideal screw propeller and an ideal turbine. The four models are presented with all relevant mathematical formulae regarding the forces, the power and the efficiency. It is demonstrated that the application of the model of an ideal optimum fluid brake according to the Betz theorem for determination of the maximum effectiveness coefficient of an axial wind turbine is not correct. In the case of a turbine the inclusion of important rotational flow losses may increase the maximum value of the turbine effectiveness coefficient above the level defined by Betz. Therefore the model of an ideal turbine should be an inversion of the model of an ideal screw propeller. This conclusion is supported by numerical calculations. It may influence the design procedures of wind turbines and may lead to increase in their efficiency.

Key words: ideal propeller, ideal wind turbine, Betz theorem, maximum efficiency

INTRODUCTION

A review of literature concerning the theory and design of wind turbines shows serious deficiencies in proper understanding and correct interpretation of the results of calculations based on modeling the flow of ideal fluid in an unbounded domain by means of principles of conservation of momentum, moment of momentum and energy. An example of this may be the maximum value of the efficiency of an ideal wind turbine, determined by Betz [1] and quoted as an absolute upper limit even in the most recent publications.

Starting from the 1960s the models of an ideal propulsor and an ideal propeller were used at Institute of Fluid Flow Machinery, e.g. for determination of the tunnel wall influence on the hydrodynamic characteristics of propellers [3] and for determination of the hydrodynamic characteristics of propellers by means of the vortex theory. The experience acquired over many years enables a thorough analysis of the applicability of the above mentioned ideal models to problems of operation of real fluid flow machines.

The principles of conservation of momentum, moment of momentum and energy in connection with the appropriate vortex models enable the determination of maximum achievable performance of certain fluid flow machines, such as:

- an ideal propulsor,
- an ideal screw propeller,
- an ideal fluid brake,
- an ideal axial wind turbine.

In the cases of an ideal propulsor and ideal fluid brake the required results may be obtained without resorting to vortex models. However, if the information about flow details in the close vicinity of the disc is required, the application of the vortex model (or the equivalent accelerating or decelerating actuator disc) is necessary. In the cases of an ideal screw propeller or an ideal turbine the application of vortex models is necessary at every stage of calculations. The detailed presentation and discussion of the computational models for all four above mentioned machines is given below.

AN IDEAL PROPULSOR

An ideal propulsor is the simplest form of the fluid propulsor, in which a surface perpendicular to the flow (not necessarily of a circular shape) covered with pressure dipoles accelerates the flow both in front and behind the propulsor (cf. Fig. 1). At the propulsor surface itself a jump in fluid pressure is created. Consequently, a propulsor stream is generated, in which at a certain distance (typically about 3 diameters of the propulsor disc) the velocity achieves constant values at the cross-sections of the stream both behind (section 3 in Fig. 1), in front of the propulsor (section 1) and on the cylindrical side surface of the stream. The sections 1 and 3 are referred to as "far in front" and "far behind" the propulsor. In reality the closest to the ideal propulsor is the magneto-hydrodynamic propulsor, used as the "silent" propulsor on some submarines. In these propulsors a strong electromagnetic field generates

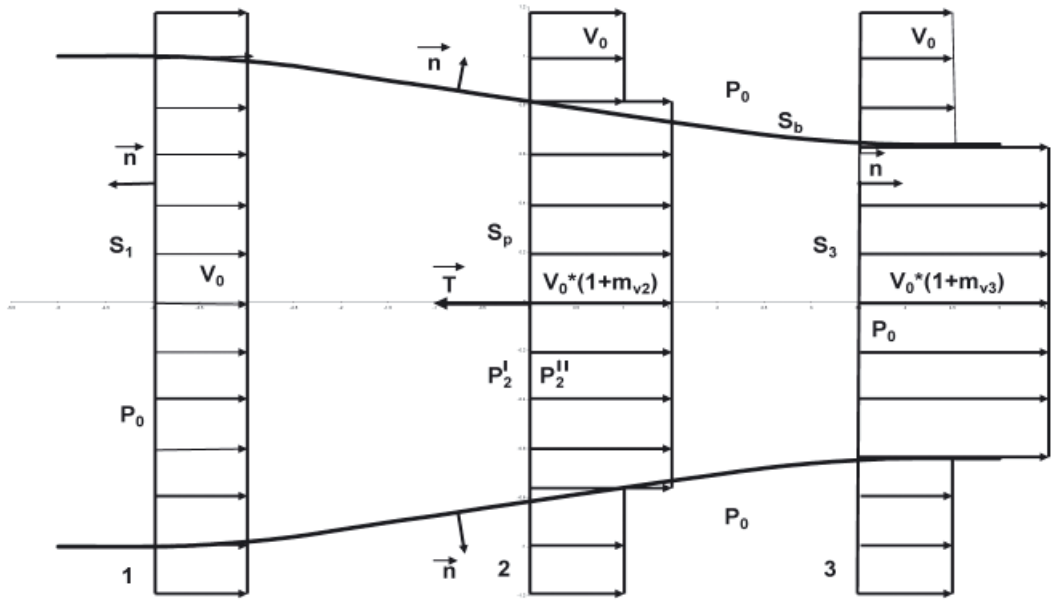

Fig. 1. *The stream of an ideal propulsor*

motion of particles of salt water. Strictly ideal case of such a propulsor would require elimination of the boundary layer on the propulsor channel walls. Within the model of an ideal propulsor two cases may be distinguished:

- an optimum ideal propulsor,
- a non-optimum ideal propulsor.

The above cases depend strictly upon the uniformity of the velocity field inside the propulsor stream. Namely, every deviation from the uniform velocity field leads to the reduction of efficiency. Further discussion is limited to the optimum case only.

In an optimum ideal propeller the axial force acting on the fluid is equal to the multiple of pressure jump and the area of the propulsor surface:

$$T = \pi R_2^2 (p_2' - p_2'') \tag{1}$$

In the case of the optimum ideal propulsor the distribution of the pressure dipoles over the propulsor surface is uniform and the pressure jump Δp may be univocally determined from the Bernoulli equation for any streamline in front and behind the propulsor (Fig. 1):

$$\tfrac{1}{2}\rho V_0^2 + p_0 = \tfrac{1}{2}\rho (V_0 + V_{x2})^2 + p_2' \tag{2a}$$

$$\tfrac{1}{2}\rho (V_0 + V_{x3})^2 + p_0 = \tfrac{1}{2}\rho (V_0 + V_{x2})^2 + p_2'' \tag{2b}$$

After subtracting (2b) from (2a) the pressure jump at the propulsor surface Δp is obtained:

$$\Delta p = p_2'' - p_2' = \rho V_0^2 m_{v3} \left(1 + \frac{1}{2} m_{v3}\right) \tag{3}$$

Substitution to formula (1) yields the thrust of the propulsor:

$$T = \rho V^2 \pi R^2 m_{v3} \left(1 + \frac{1}{2} m_{v3}\right) \tag{4}$$

where:
$m_{v3} = V_{x3}/V_0$

The ideal thrust loading coefficient of the propulsor is equal to:

$$C_{T2i} = \frac{T}{\left(\frac{1}{2}\rho V_0^2 \pi R^2\right)} = 2 m_{v3} \left(1 + \frac{1}{2} m_{v3}\right) \tag{5}$$

The thrust of the propulsor may be also obtained from the momentum conservation principle applied to the control surface S consisting of the side surface of the stream S_b, inlet cross-section of the stream S_1, outlet cross-section of the stream S_3 and the surface containing the external forces acting on the fluid S_p (Fig. 1):

$$\int_S \rho \vec{V} (\vec{V} \cdot \vec{n}) dS = -\int_S p \vec{n} dS \tag{6}$$

If the surface S_p, encompassing the external forces, is excluded from the surface S, then the axial force (thrust) T is equal to the rate of change of fluid momentum on the entire control surface and the force induced by the pressure field on the remaining part of S:

$$T = -\int_{Sp} p \vec{n} dS = \int_S \rho \vec{V} (\vec{V} \cdot \vec{n}) dS + \int_{S-Sp} p \vec{n} dS \tag{7}$$

On the surface S_1 there is $\vec{V} \cdot \vec{n} = -V_0$ and on the surface S_3 there is $\vec{V} \cdot \vec{n} = V_0 + V_{x3}$. Consequently, the following relation between S_1 and S_3 may be established, making use of the continuity equation:

$$\pi R_1^2 V_0 = \pi R_3^2 (V_0 + V_{x3}) \tag{8}$$

In the case of an unbounded fluid domain the same pressure p_0 acts on the entire surface S including surfaces S_1, S_b and S_3, hence the second term in equation (7) is zero. In case of a bounded fluid domain (e.g. inside a tunnel) this condition does not hold.

Taking into account that the side surface of the propulsor stream is in fact the stream surface, the scalar multiple $\vec{V} \cdot \vec{n} = 0$. Finally, another formula for the axial force (or thrust) induced by an ideal propulsor is obtained:

$$T = \rho V_0^2 \pi R_3^2 m_{v3} (1 + m_{v3}) \tag{9}$$

Comparing formulae (9) and (4), the relation between the velocities induced at the propulsor and "far behind" the propulsor is obtained:

$$\frac{\pi R_2^2}{\pi R_3^2} = \frac{1 + \frac{1}{2} m_{v3}}{1 + m_{v3}} \tag{10}$$

It may be concluded from this relation that the induced velocity at the propulsor is equal half of the value of the

induced velocity "far behind". Often this relation is accepted "a priori", which is not always correct, because it depends on the above assumptions, regarding an unbounded fluid domain and uniformity of velocity distribution over the propulsor surface.

The thrust loading coefficient of the propulsor, related to the area of the propulsor stream cross-section "far behind" the propulsor is equal to:

$$C_{T3i} = \frac{T}{\frac{1}{2}\rho V_0^2 \pi R_3^2} = 2m_{v3}(1+m_{v3}) \tag{11}$$

The following relation stems from the principle of energy conservation (disregarding heat exchange):

$$P_D = \int_S p\vec{V}\cdot\vec{n}dS + \frac{1}{2}\rho\int_S V^2(\vec{V}\cdot\vec{n})dS \tag{12}$$

The scalar multiple on the side surface of the propulsor stream $\vec{V}\cdot\vec{n}=0$. The sum of integrals on the surfaces S_1 and S_3 is also equal zero according to the continuity equation:

$$\int_{S1} p_0 V_1 dS - \int_{S3} p_0 V_3 dS = p_0(V_1S_1 - V_3S_3) = 0$$

Hence the power (energy per second) lost in the stream is equal to:

$$P_{Di} = \frac{1}{2}\rho\int_S V^2(\hat{V}\cdot\vec{n})\,dS = \rho V_0^3\pi R_3^2\left(\left(\frac{V_{x3}}{V_0}\right)^3 - \frac{S_1}{S_3}\right) = \tag{13}$$

$$= \rho V_0 \pi R_3^2 m_{v3}(1+m_{v3})\left(1+\frac{1}{2}m_{v3}\right)$$

The power loading coefficient of the propulsor, related to the area of the propulsor stream cross-section "far behind" the propulsor is equal to:

$$C_{p3i} = \frac{P_{Di}}{\frac{1}{2}\rho V_0^3 \pi R_3^2} = 2m_{v3}(1+m_{v3})\left(1+\frac{1}{2}m_{v3}\right) \tag{14}$$

The same coefficient related to the propulsor surface area is equal to:

$$C_{p2i} = \frac{P_{Di}}{\frac{1}{2}\rho V_0^3 \pi R_2^2} = 2m_{v3}\left(1+\frac{1}{2}m_{v3}\right)^2 \tag{15}$$

The efficiency of the propulsor is defined as the ratio of the power of thrust to the power lost at the cross-section "far behind" the propulsor (cf. Fig. 2):

$$\eta_i = \frac{T_i V_0}{P_{Di}} = \frac{C_{T3i}}{C_{P3i}} = \frac{1}{1+\frac{1}{2}m_{v3}} \tag{16}$$

The efficiency of an ideal propulsor is often presented as a function of the thrust loading coefficients C_{T3i} or C_{T2i}.

Using the formula (11) a quadratic equation may be solved, leading to the following relation:

$$m_{v3} = \frac{1}{2}\left(\sqrt{1+2C_{T3i}} - 1\right) \tag{17}$$

which in turn may be used to develop the following formula for propulsor efficiency, depending on the thrust loading coefficient "far behind":

$$\eta_i = \frac{4}{3+\sqrt{1+C_{T3i}}} \tag{18}$$

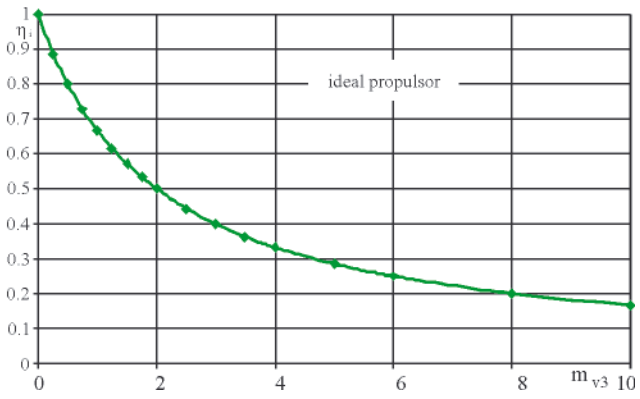

Fig. 2. The dependence of the ideal propulsor efficiency on the relative induced velocity "far behind" the propulsor

In the case when the thrust loading coefficient at the propulsor surface is available, this relation takes a different form:

$$\eta_i = \frac{2}{1+\sqrt{1+C_{T2i}}} \tag{19}$$

Fig. 3 shows the dependence of the ideal propulsor efficiency on the thrust loading coefficients determined at the propulsor and "far behind".

The above formulae refer to the optimum ideal propulsor, i.e. a propulsor operating in an unbounded fluid domain and having uniform distribution of thrust loading at its surface. When these assumptions are not fulfilled (this was the case of determination of the tunnel walls influence on the propulsor characteristics, as described in [3]), the induced velocity at the propulsor is no longer equal to half of the value of this velocity "far behind". The deviation from this depends on the degree on non-uniformity of the thrust loading and on the ratio of the propulsor surface to the cross-section of the bounded fluid domain [3]. The vortex model of an ideal propulsor is composed of circular vortices distributed on the side surface of the propulsor stream behind the propulsor surface.

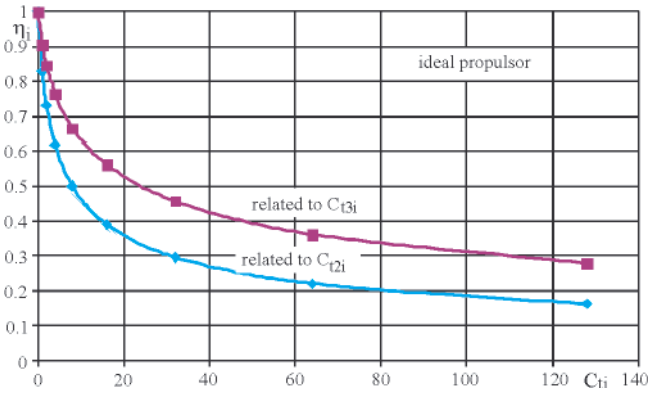

Fig. 3. The ideal propulsor efficiency as the function of thrust loading coefficients

AN IDEAL FLUID BRAKE

Physically an ideal fluid brake operates in the manner similar to an ideal propulsor, but now the pressure dipoles are directed in an opposite direction, i.e. against the direction of flow. Hence instead of an accelerating surface, there is now a decelerating surface and the axial force is generated in an opposite direction. The flow velocity is being reduced both in front and behind the brake surface (cf. Fig. 4). Similarly as before, the principles of momentum and energy conservation may be used for determination of the axial force and power. The

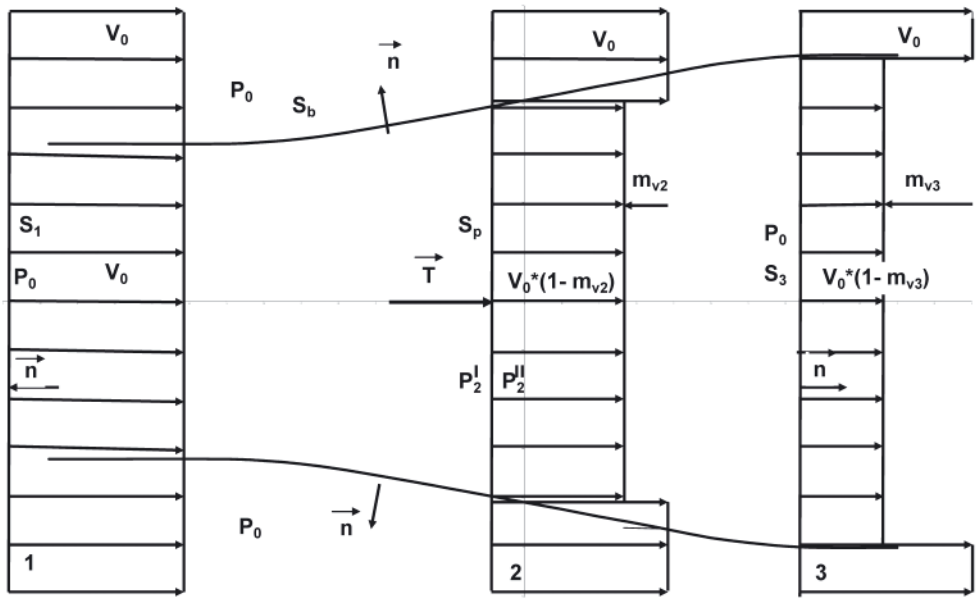

Fig. 4. The stream of an ideal fluid brake

formulae are similar to those describing the propulsor, only the signs of induced velocity are changed and certain limitations in the values of these velocities are introduced.

The axial force (now named the braking force instead of thrust) coefficient related to the stream cross-section "far behind" is now equal to:

$$C_{T3i} = -2m_{v3}(1-m_{v3}) \tag{20}$$

and the coefficient of power loss in the stream, also related to the cross-section "far behind" is equal to:

$$C_{P3i} = -2m_{v3}(1-m_{v3})\left(1-\frac{1}{2}m_{v3}\right) \tag{21}$$

Similarly as in the case of a propulsor, for the brake operating in an unbounded fluid domain and having uniform loading distribution over its surface, the velocity induced at the decelerating surface is equal to half the velocity induced at the cross-section "far behind" the brake. Hence the ratio between the areas of the brake surface and the stream cross-section "far behind" may be obtained from the continuity principle:

$$\frac{\pi R_3^2}{\pi R_2^2} = \frac{1-\frac{1}{2}m_{v3}}{1-m_{v3}}$$

Consequently, the coefficients of axial force and power loading, related to the brake area, have now the following form:

$$C_{T2i} = -2m_{v3}\left(1-\frac{1}{2}m_{v3}\right) \tag{22}$$

$$C_{P2i} = -2m_{v3}\left(1-\frac{1}{2}m_{v3}\right)^2 \tag{23}$$

The functions showing the dependence of the above coefficients on the induced velocity are plotted in Figs 5 and 6. The range of variation of the relative induced velocity "far behind" was limited to 1.0, because larger values would lead to physically unrealistic reversed flows.

In case of a fluid brake it is inconvenient to discuss its "efficiency". The more appropriate parameter is its effectiveness. For example the ratio of the braking force power to the power loss in the brake stream may be proposed as the measure of the brake effectiveness:

$$\zeta = \frac{T \cdot V_0}{P_{D2I}} = \frac{C_{T2i}}{C_{P2i}} = \frac{1}{1-\frac{1}{2}m_{v3}} \tag{24}$$

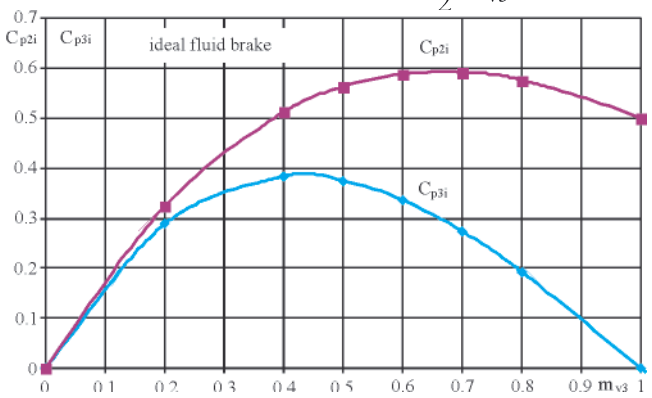

Fig. 5. Coefficients of kinetic energy loss in the brake stream depending on the relative induced velocity "far behind" m_{v3}

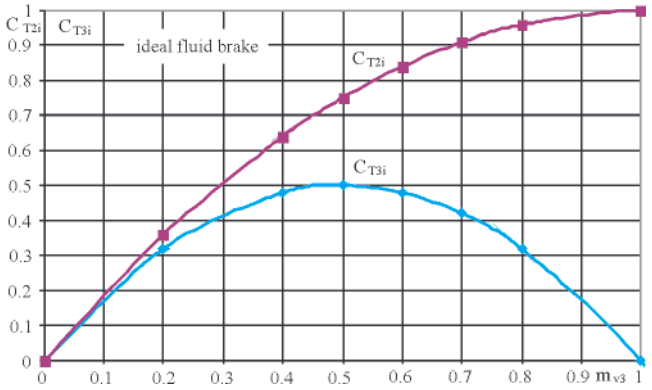

Fig. 6. Coefficients of the braking force depending on the relative induced velocity "far behind" m_{v3}

The value of the above parameter varies from 1.0 for m_{V3} = = 0.0 to 0.5 for m_{V3} = 1.0 . The above presented formulae contain all relations between kinematic and dynamic parameters of an ideal brake.

It must be stressed here, that it is not correct to identify the value of C_{P2i} determined by the formula (23) with the ideal efficiency coefficient for the axial wind or water turbines. This was suggested by Betz [1], who has used formula (23) for determination of the maximum ideal efficiency

of a wind turbine (cf. Fig. 5). According to his result, quoted in almost all publications concerning wind turbines, this maximum value is equal to $C_{pmax} = 16/27 = 0.5926$, which is obtained for: $m_{V3} = 2/3 = 0.6667$.

Contrary to the above, in experiments with real turbines having finite number of blades and operating in a real, viscous fluid (e.g air or water) significantly higher values of C_{P2} are obtained. This results from the fact that **the operation of an ideal axial turbine should be determined not on the basis of the ideal fluid brake, but in the way similar to that presented below for an ideal screw propeller.** The power of a turbine depends on the torque on its shaft and consequently, the **circumferential induced velocity** must be taken into account. In this case the principle of conservation of moment of momentum is more appropriate for determination of torque on the turbine shaft and the performance of the turbine should be made dependent on a parameter characterizing the moment of momentum.

The energy conservation principle, taking into account all components of the induced velocities may also be used, but this way of solving the problem is much more difficult and less clear. Both ways lead to the same final result.

AN IDEAL SCREW PROPELLER

An ideal screw propeller model takes into account the rotational motion, therefore it must have a form of a circular disc. In order to determine the relations between the induced velocities and the forces on an ideal screw propeller, a more complicated vortex model should be used (cf. Fig. 7).

This model is constructed of:

- straight line vortices distributed radially on the propeller disc,
- helicoidal tip vortex lines distributed over the cylindrical side surface of the propeller stream behind the propeller,
- straight line vortex located along the propeller axis behind the propeller, having the total intensity Γ,

The velocity field induced by such a vortex system at a certain distance behind the propeller (practically about one propeller diameter is enough) may be univocally determined by the parameters of the vortex system "far behind" the propeller. These parameters are:

- radius of the cylinder on which the helicoidal vortices are distributed "far behind" R_3,
- total intensity of the vortices Γ,
- velocity of the undisturbed flow V_0,
- pitch of the helicoidal vortex lines $\tan\beta_3$

The volumetric mean value of the axial velocity induced inside the stream ($r < R_3$) by the system of infinite helicoidal vortices has a constant value across the stream [4], equal to:

$$V_{xi3} = \Gamma/(2\,\pi\,R_3\,\tan\beta_3) \tag{25}$$

This value applies to a single helicoidal vortex line as well as to a system of Z (including $Z = \infty$) heilcoidal lines having the same pitch equal to $\tan\beta_3$, as long as the total intensity of all vortex lines is equal to Γ. At the same time the volumetric mean velocity induced outside the stream ($r > R_3$) is equal zero [4].

The volumetric mean circumferential velocity induced inside the propeller stream ($r < R_3$) by the infinite straight line vortex located at the propeller axis is equal to:

$$V_{\varphi i3} = \Gamma/(2\,\pi\,r) \tag{26}$$

The volumetric mean of the circumferential velocity induced by the system of tip vortices inside the stream ($r < R_3$) is equal zero, while this value outside the stream ($r > R_3$) is determined by the formula (25) with inverted sign due to inverted direction of the tip vortices. Consequently, outside the stream the volumetric mean of the circumferential velocity induced by the entire vortex system of the propeller (axial vortex together with tip vortices) is equal zero. The volumetric mean of the radial component of the induced velocity "far behind" the propeller is equal zero both inside and outside the propeller stream.

When the non-dimensional value of the intensity of vortices forming the propeller vortex system is introduced as:

$$b_{V3} = \Gamma/(4\,\pi\,R_3\,V_0) \tag{27}$$

the relative values (divided by the undisturbed flow velocity V_0) of the induced velocity components may be expressed by the following formulae:

$$V_{xi3}/V_0 = m_{V3} = 2\,b_{V3}/\tan\beta_3 \tag{28}$$

$$V_{\varphi i3}/V_0 = 2\,b_{V3}/r = m_{V3}\tan\beta_3/r \tag{29}$$

When the velocity field "far behind" the propeller is defined in the above way, the relations between this field and propeller thrust T, torque Q and power loss may be developed

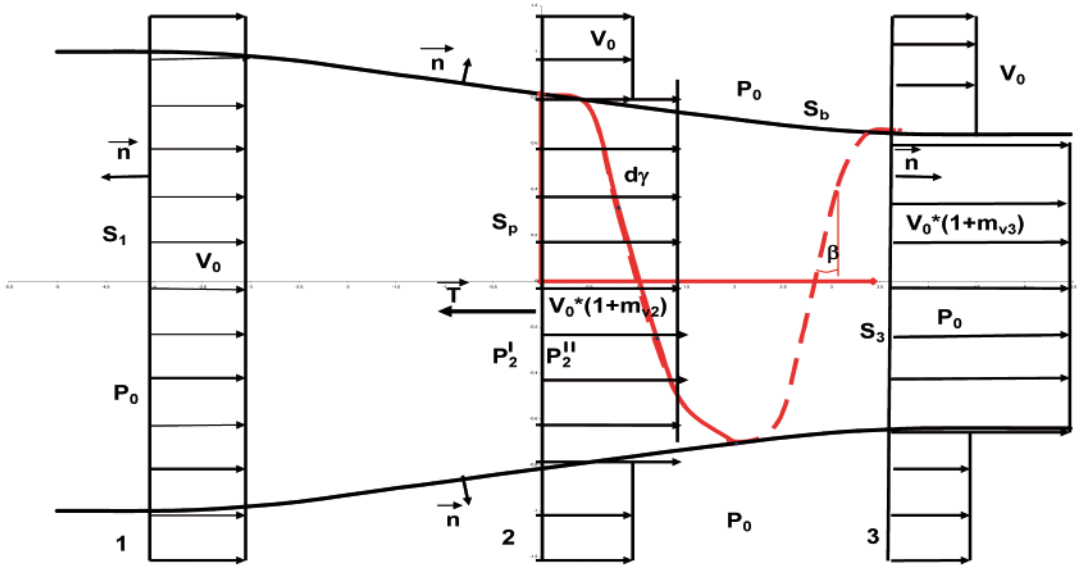

Fig. 7. The stream of an ideal screw propeller with vortex lines

similarly as for an ideal propulsor, making use of the principles of conservation of momentum, moment of momentum and energy.

It may seem that due to the constant value of the axial induced velocity across the stream, the value of propeller thrust may be determined analogically as in the case of an ideal propulsor. Unfortunately, the presence of the axial hub vortex significantly changes the pressure field inside the stream. Therefore, the thrust must be determined on the basis of the momentum conservation principle applied to the control surface S, which includes the side surface of the stream S_b, inlet and outlet surfaces S_1 and S_3 together with the surface encompassing the external forces acting on the fluid Sp (cf. Fig. 7).

$$\int_S \rho\vec{V}(\vec{V}\cdot\vec{n})\,dS = -\int_S p\vec{n}dS \tag{30}$$

If the surface S_p (representing the blades of the propeller) is excluded from the control surface S, then the thrust is equal to the rate of change of fluid momentum on the entire control surface and the force generated by the pressure field on the remaining part of S:

$$T = -\int_{Sp} p\vec{n}dS = \int_S \rho\vec{V}(\vec{V}\cdot\vec{n})\,dS + \int_{S-Sp} p\vec{n}dS \tag{31}$$

As there is $\vec{V}\cdot\vec{n} = -V_0$ in cross-section 1 and there is $\vec{V}\cdot\vec{n} = V_0 + V_{x3}$ in cross-section 3, the relation between areas of cross-sections 1 and 3 may be determined using the principle of continuity of flow. However, it should be taken into account that on the axis of cross-section 3 there exists a vortex line, which should be treated as a vortex singularity (e.g. a Rankine vortex model), having cross-section area S_w and radius R_{wo}.

$$(S_3\text{-}S_w)\,(V_0+V_{x3}) = S_1\,V_0 \tag{32}$$

In the case of an ideal propulsor discussed above the same pressure p_0 acts on the entire control surface S (assuming unbounded fluid domain). In the case of ideal screw propeller the pressure in cross-section S_3 is different than p_0 and it is a function of radius, therefore an additional pressure term must appear in the corresponding equation. The side surface of the propeller stream is still a stream surface, where $\vec{V}\cdot\vec{n} = 0$. Taking into account the above, the relation (31) now takes the following form:

$$T = \rho\pi R_3^2 V_{x3}(V_0 + V_{x3})(S_3 - S_w) + \int_{S3}(p - p_0)dS \tag{33}$$

Substituting the relative induced velocity, this may be transformed into:

$$T = \rho V_0^2\pi R_3^2 m_{v3}(1+m_{v3})(1-(R_w/R_3)^2) + \int_{S3}(p-p_0)dS \tag{34}$$

The first term of (34) is similar to the corresponding term in the formula (9) for an ideal propulsor. Calculation of the second term requires additional assumptions:

- the entire vorticity in the flow is concentrated in the limited space around the tip and axial vortices; outside this limited space the flow is irrotational i.e. potential,
- according to Joukovsky hypothesis the flow is steady in the system of co-ordinates rotating with the propeller.

In such a situation the following relation exists between the velocity field and the pressure field:

$$1/2V^2 - \vec{V}\bullet\vec{V}_e + p/\rho = \text{const} \tag{35}$$

where:
$\vec{V}_e = \vec{\omega}\times\vec{R}$ – the convective velocity ($\vec{\omega}$ is the angular propeller velocity), hence:

$$p - p_0 = 1/2\,\rho(V_{xi}^2 + V_{\varphi i}^2) + \rho(V_{xi}V_0 - \varpi\cdot r\cdot V_{\varphi i}) \tag{36}$$

Taking into account the equations (28) and (29) and reformulating the equation (36), the following equation for the thrust correction resulting from the pressure field in the screw propeller stream may be obtained:

$$\int_{S3}(p-p_0)dS = 1/2\,\rho V_0^2 m_{V3}^2 2\pi R_3^2\int_{rw}^{1}(1+\tan\beta_3^2/r_z^2)r_z dr_z + \rho V_0^2 m_{V3} 2\pi R_3^2\int_{rw}^{1}(1-r_z\tan\beta_3/\lambda_3)r_z dr_z \tag{37}$$

where:
$r_z = r/R_3$
$\lambda_3 = V_0/\varpi R_3$
$r_w = R_w/R_3$ is the normalized radius of the axial vortex

The above integrals may be solved analytically and ultimately they lead to the formula for the thrust of an ideal screw propeller:

$$T = \rho V_0^2\pi R_3^2 m_{v3}((1+m_{v3})(1-r_w^2) + \tfrac{1}{2}\,m_{V3}\tan\beta_3^2(2\ln(r_w)+1-r_w^2)) \tag{38}$$

Now the thrust loading coefficient related to the propeller stream cross-section "far behind" is equal to:

$$C_{T3i} = \frac{T}{\frac{1}{2}\rho V_0^2\pi R_3^2} = 2m_{v3}((1+m_{v3})(1-r_w^2) + \frac{1}{2}\,m_{V3}\tan\beta_3^2(2\ln(r_w)+1-r_w^2)) \tag{39}$$

The power loading coefficient, related to the screw propeller stream cross-section "far behind", may be determined from the principle of conservation of moment of momentum. In this case only the circumferential component of the induced velocity is important. This leads to the formula:

$$Q_{xi} = \int_{S-S_p}\rho(\overline{P}\vec{O}\times\vec{V})_x(\vec{V}\cdot\vec{n})dS + \int_{S-S_p} p(\overline{P}\vec{O}\times\vec{n})_x dS \tag{40}$$

where:
$\overline{P}\vec{O}$ – radius-vector from propeller axis
$\vec{n}$ – unit normal vector at the control surface S-Sp

An appropriate selection of the control surfaces enables elimination of some of the integrals. On the entire surface S-Sp the vector multiple $(\overline{P}\vec{O}\times\vec{n})_x$ is zero, eliminating the pressure term. On the stream surfaces the scalar multiple $\vec{V}\cdot\vec{n}$ is zero. On the cross-section S1 the following relations hold:

$$\vec{V}\cdot\vec{n} = -V_0$$

$$(\overline{P}\vec{O}\times\vec{n})_x = [\overline{P}\vec{O}\times(-\vec{n}\cdot V_0)] = 0$$

$$(\vec{n})_x = -1$$

and on the cross-section S_3 the following relations hold:

$$\vec{V}\cdot\vec{n} = V_0 + V_{x3}$$

$$(\overline{P}\vec{O}\times\vec{n})_x = \overline{P}\vec{O}\cdot V_{\varphi 3}$$

$$(\vec{n})_x = 1$$

Taking the above into account, together with the continuity equation, the following is obtained:

$$Q_{xi} = \rho \int_{S_3 - S_w} r_z V_{\varphi 3}(1+V_{x3})\,dS \tag{41}$$

After substituting the expressions (28) and (29) for the components of the induced velocity, the following equation is obtained for the power of an ideal screw propeller:

$$P_i = Q_{xi}\cdot\omega_0 = \\ = \rho V_0^3 \pi R_3^2 \tan\beta_3/\lambda_3\, m_{V3}(1+m_{V3})(1-r_w^2) \tag{42}$$

where:
$\lambda = V_0/(\omega_0 R_3)$

The power loading coefficient, related to the area of the propeller stream cross-section "far behind", may be now determined as:

$$C_{Pi} = P_i/\frac{1}{2}\rho V_0^3 \pi R_3^2 = \\ = 2\tan\beta_3/\lambda_3\, m_{V3}(1+m_{V3})(1-r_w^2) \tag{43}$$

The efficiency of an ideal propeller is defined as the ratio of the power of thrust to the power loss in the propeller stream "far behind" the propeller:

$$\eta_i = \frac{T_i V_0}{P_{Di}} = \\ = (1+1/2\, m_{V3}\tan\beta_3^2(2\ln(r_w)+1-r_w^2))\lambda_3/\tan\beta_3 \tag{44}$$

The formula (44) does not resemble the formula (16) for the efficiency on an ideal propulsor. However, it is similar to the formula used in the vortex theory of propellers for determination of the so called induced pitch for the propeller blades having optimum radial distribution of circulation:

$$tg\beta = \lambda/\eta \tag{45}$$

where:
$\lambda = V_0/\omega R$

The formula (44) may take the form similar to formula (16) if the following definition of $\tan\beta_3$ is used:

$$\tan\beta_3 = \frac{V_0 + V_{xw}}{\omega R_3 - V_{\varphi w}} = \frac{1+1/2m_{V3}}{1/\lambda_3 - 1/2 m_{V3}\tan\beta_3} \tag{46}$$

where:
V_{xw} and $V_{\varphi w}$ – the components of the own velocity of the tip vortex. For an ideal propeller they are equal half of these components induced inside the propeller stream [4]. After some reformulations the following equation is obtained:

$$\lambda_3/\tan\beta_3 = \frac{1}{1+1/2 m_{V3}(1+\tan\beta_3^2)} \tag{47}$$

After substitution of (47) into (45) the formula similar to that for the efficiency of an ideal propulsor is obtained:

$$\eta_i = \frac{T_i V_0}{P_{Di}} = \frac{1+1/2\, m_{V3}\tan\beta_3^2(2\ln(r_w)+1-r_w^2)}{1+1/2 m_{V3}(1+\tan\beta_3^2)} \tag{48}$$

The formula (48) differs from the formula (16) in two aspects:
- the numerator is smaller than 1
- the denominator includes an additional factor

Both these differences cause reduction of the ideal propeller efficiency in comparison with an ideal propulsor. Therefore, the efficiency of an ideal screw propeller is always smaller than that of a corresponding ideal propulsor. Moreover, the ideal screw propeller efficiency depends additionally on the pitch of the helical vortex lines and on the diameter of the axial vortex singularity. Both formulae coincide when $\tan\beta_3 = 0$. In this case the helical vortices of an ideal propeller are reduced to the ring vortices of an ideal propulsor.

The radius of the axial vortex singularity requires further explanation. In case of an ideal screw propeller operating in water the cavitating vortex kernel may determine this radius. In case of an ideal screw propeller operating in gas (e.g. in air), there exists an exact relation between the pressure and volume (or density) based on a perfect gas model. In this case the axial vortex may be treated as a perfect whirlwind having a kernel of zero vorticity. The radius of such a kernel may be substituted into all above formulae in the place of rw.

AN IDEAL AXIAL WIND TURBINE

Similarly as in the case of an ideal propulsor and ideal brake, there exists a close analogy between an ideal screw propeller and an ideal axial wind turbine. Namely, they both may be described by the formulae characterizing the vortex system "far behind":
- radius of the cylindrical propeller stream "far behind" R_3,
- total intensity of the vortices Γ,
- undisturbed flow velocity V_0,
- pitch of the helical vortex lines $\tan\beta_3$.

The vortex system of an ideal axial turbine, shown in Fig. 8, is composed of the same elements as the corresponding system for an ideal propeller:
- straight line vortices distributed radially on the propeller disc,
- helicoidal tip vortex lines distributed over the cylindrical side surface of the turbine stream behind the turbine,
- straight line vortex located along the turbine axis behind the turbine, having the total intensity Γ.

Of course it must be remembered that the vorticity vectors for the propeller and for the turbine have opposite direction.

In this case the velocity field is related to the parameters of the vortex system in the same way as in the ideal screw propeller. The relations (25) – (29) have the same form, but the parameters mv have opposite sign. The relations for the axial force T (38) and for the power Pi (42) have the same form, but the sign of m_{v3} is changed:

$$T = -\rho V_0^2 \pi R_3^2 m_{V3}((1-m_{V3})(1-r_w^2) + \\ - \tfrac{1}{2} m_{V3}\tan\beta_3^2(2\ln(r_w)+1-r_w^2)) \tag{49}$$

$$P_{3i} = Q_{xi}\cdot\omega_0 = \\ = -\rho V_0^3 \pi R_3^2 \tan\beta_3/\lambda_3\, m_{V3}(1-m_{V3})(1-r_w^2) \tag{50}$$

The definitions of all parameters are the same as for an ideal screw propeller. Consequently, the formulae for the coefficients

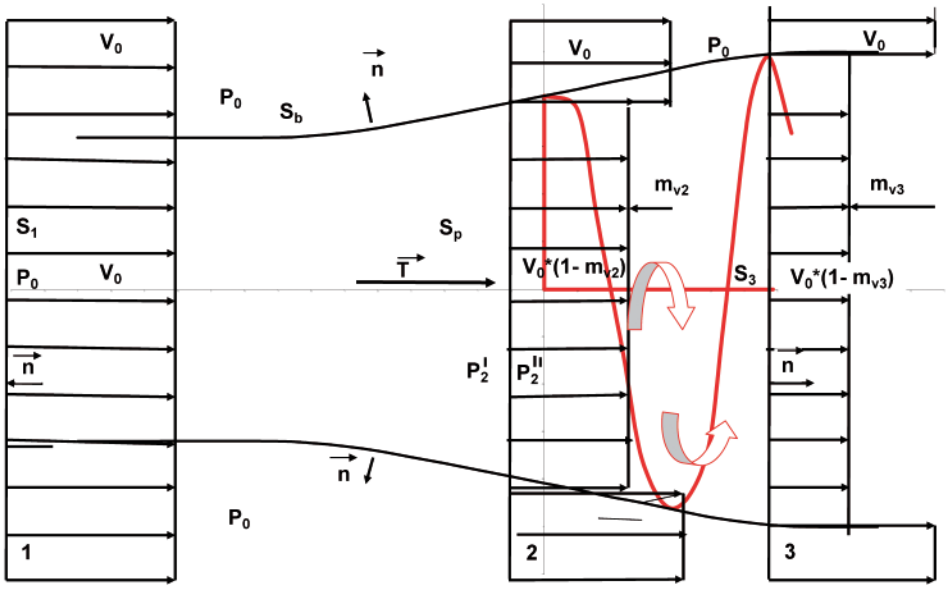

Fig. 8. The stream of an ideal axial turbine with vortex lines

of axial force loading C_{T3} and power loading C_{P3} are similar to those for an ideal propeller:

$$C_{T3i} = \frac{T}{\frac{1}{2}\rho V_0^2 \pi R_3^2} = -2m_{v3}((1-m_{v3})(1-r_w^2)+ \tag{51}$$

$$-1/2\, m_{V3} \tan\beta_3^2 (2\ln(r_w)+1-r_w^2))$$

$$C_{P3i} = P_i / 1/2\,\rho V_0^3 \pi R_3^2 = \tag{52}$$

$$= -2\tan\beta_3/\lambda_3\, m_{V3}(1-m_{V3})(1-r)$$

But now the formula for the pitch of the helical lines $\tan\beta_3$ does change into:

$$\tan\beta_3 = \frac{V_0 + V_{xw}}{\omega R_3 - V_{\varphi w}} = \frac{1-1/2m_{V3}}{1/\lambda_3 + 1/2m_{V3}\tan\beta_3} \tag{53}$$

from which the following relation may be developed:

$$\tan\beta_3/\lambda_3 = 1\text{-}1/2m_{v3}(1+\tan^2\beta_3) \tag{54}$$

Taking into account the formula (54) the relation (52) may be transformed into the form similar to (21):

$$C_{p3i} = \text{-}2\ m_{v3}\ (1\text{-}m_{v3})(1\text{-}1/2m_{v3}(1+\tan^2{}_{b3}))(1\text{-}r_w{}^2) \tag{55}$$

In this way it may be proved that in the system dependent on the axial component of the induced velocity $m_{v3,}$ the limiting maximum values of the power coefficient C_{p3i} are even smaller than for the ideal fluid brake (assuming that $\tan\beta_3 = 0$ corresponds to the brake model and leads to the formula (21)).

Taking into account that the axial velocity component is only weakly related to the moment of momentum (i.e. to the turbine torque) and that the model experiments indicate values of C_p higher than those obtained from the ideal fluid brake, the analysis of the turbine operation should be performed in another system of co-ordinates. For example, the coefficient b_v more closely characterizes the moment of momentum in the flow.

Considering the definition formula for $m_{v3,}$ the formula for C_{P3i} takes the form:

$$C_{P3i} = P_i / 1/2\,\rho V_0^3 \pi R_3^2 = \tag{56}$$

$$= -4\, b_{V3}/\lambda_3\,(1-2b_{V3}/\tan\beta_3)(1-r_w^2)$$

As in the case of a turbine the efficiency is not defined in the same way as in the case of propeller, the above formulae complete the relations between the dynamic and kinematic parameters. The radius of the vortex singularity may be determined in the above described way. Taking into consideration the continuity equation in the stream behind the turbine, the power loading coefficient at the turbine may be easily determined:

$$C_{P2i} = P_i / 0.5\,\rho V_0^3 \pi R_2^2 = \tag{57}$$

$$= -4\, b_{V2}/\lambda_2\,(1-2b_{V2}/\tan\beta_2)(1-r_w^2)$$

This power loading coefficient is in fact the effectiveness of utilization of the energy of the oncoming flow by the turbine. The formula (56) enables further analysis of the influence of different parameters on the turbine efficiency described by C_{P3i}:

- the parameter $(1 - r_w)$, characterizing the vortex singularity, has little influence on the turbine efficiency,
- the parameter $b_{v2} = \Gamma/4\pi V_0 R_2$ characterizes the circulation of the axial vortex and the moment of momentum in the stream. This is a very important parameter, which determines the torque and power of the turbine,
- the parameter $\tan\beta_2$ characterizes the pitch of the tip vortex lines at the turbine, which is difficult to be determined precisely,
- the parameter λ_2 characterizes the location of the turbine operating point on the co-ordinate of the advance coefficient J.

It is difficult to determine the maximum attainable value of C_{P2i} using the formula (57) and the above parameters. Clearly, it will be not equal to the Betz limiting value of Cpmax = 0.5926, determined for an ideal fluid brake.

The structure of formula (57) implies that the maximum values of Cp are attained when:

- the parameter λ_2 reaches minimum values,
- the parameter Γ describing circulation of the hub vortex, corresponding to b_v, reaches the highest values,

Quantitative determination of these parameters is difficult. Certain idea of this aspect may be drawn from the analysis of the results of calculations for wind turbines with finite number of blades presented in the next section.

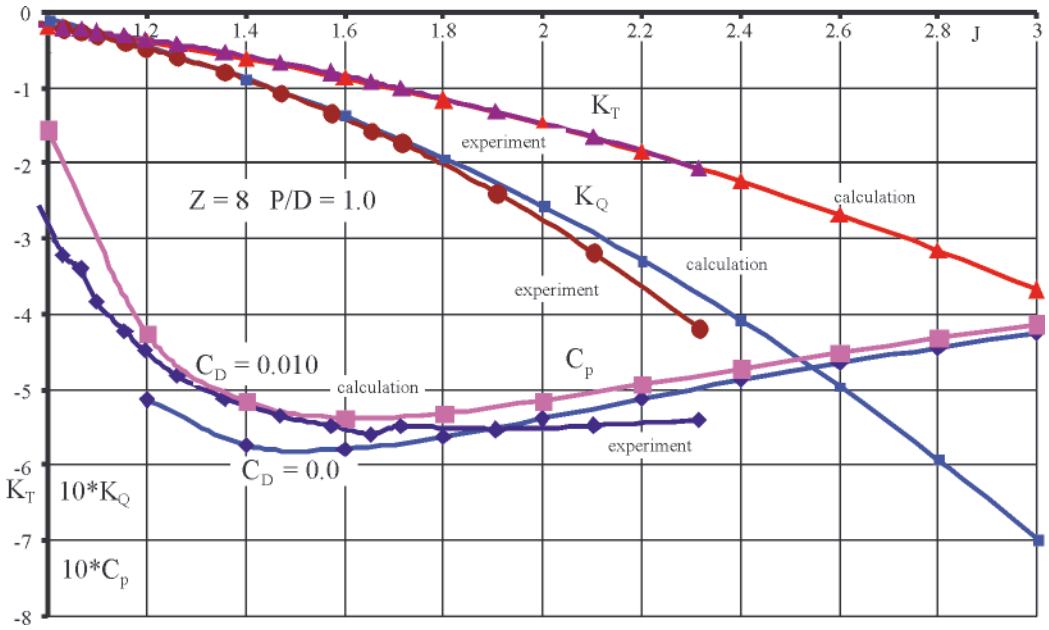

Fig. 9. *Experimental verification of the program CHAHYD in application to wind turbines*

AN AXIAL WIND TURBINE WITH THE FINITE NUMBER OF BLADES

Results of calculations showing that the effectiveness of a real axial wind turbines C_{pi} may exceed the upper limit defined by Betz have been obtained already in the 1990s, when the computer program for calculation of ship propeller characteristics CHAHYD was adapted for calculations of the axial wind turbines.

The program CHAHYD, based on the vortex lifting surface theory, was very thoroughly verified experimentally in its application to ship propellers. Similar verification with respect to wind turbines was missing until 2010 [2]. Fig. 9 shows an example of such verification. In this figure the coefficients of power loading C_p, axial force K_T, torque K_q obtained experimentally and computed for an 8-bladed turbine, are shown as functions of the advance coefficient J. In this figure the curve C_p calculated for zero drag coefficient is also plotted. In this case the maximum value $C_p = 0.58$ is already close to the limiting value determined by Betz.

The experimentally verified results of calculations are used to formulate the following statement:

The limiting value $C_{pmax} = 16/27 = 0.5926$ as determined by Betz for an ideal brake may take significantly higher values for an ideal axial turbine.

In the following figures the results of calculations of a 8-bladed wind turbine have been shown for four cases:

- model wind turbine having pitch coefficient P/D = 1.0 and viscous drag coefficient $C_D = 0.010$ (these results are correlated with model experiments [2]),
- the same model with P/D = 1.0 but with zero viscous drag,
- the model with pitch reduced to P/D = 0.8 and zero viscous drag ($C_D = 0.0$),
- the model with pitch reduced to P/D = 0.6 and zero viscous drag ($C_D = 0.0$).

As may be seen in Fig. 11 for the blade pitch P/D = 0.8 the C_{pmax} value already exceeds the Betz maximum of 0.5926. Still higher values of C_{pmax} are obtained for a turbine with P/D = 0.6. If such values are obtained for a real wind turbine operating

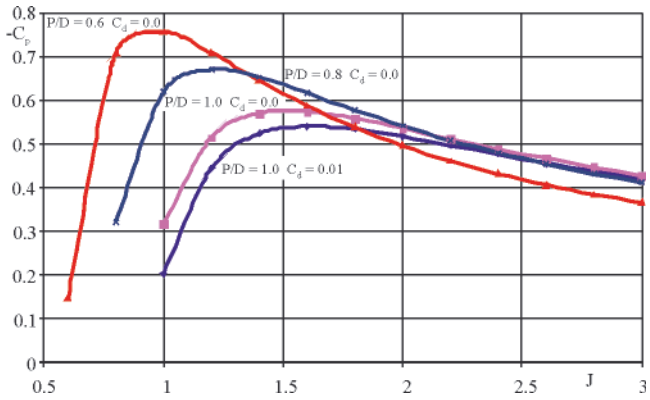

Fig. 10. *Results of calculations of the effectiveness C_p for an 8 bladed wind turbine*

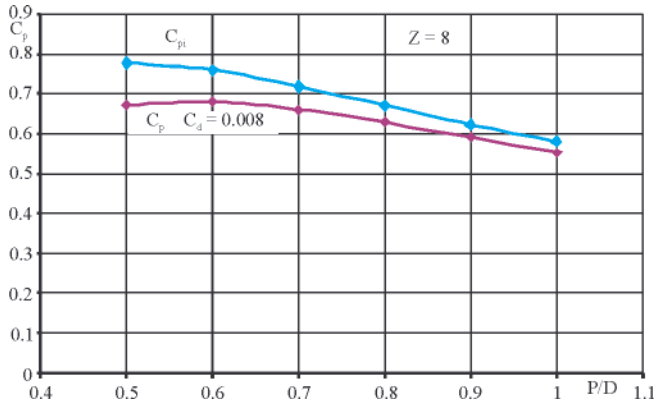

Fig. 11. *Calculated maximum values of C_p obtained with viscous drag coefficients $C_d = 0.008$ and $C_d = 0.0$ as functions of the turbine pitch coefficient P/D*

in a viscous flow and having finite number of blades, then the corresponding values for an ideal wind turbine must be even higher. In Fig. 12 the results for wind turbines having different numbers of blades are presented.

The quantitative assessment of terms in equation (57) is difficult because the vortex model of a wind turbine with finite number of blades is markedly different from the ideal turbine with infinite number of blades. First of all, the fields of induced velocity are different and the limits of the turbine

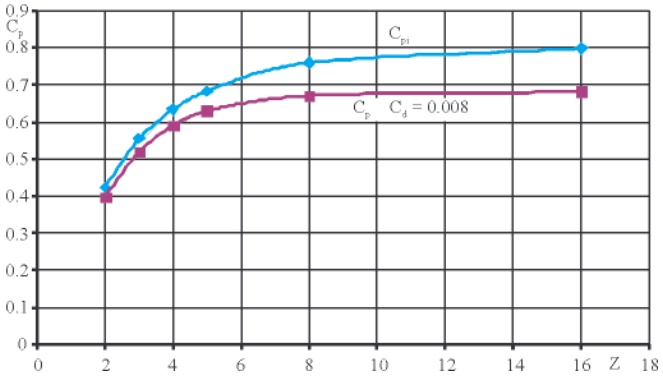

Fig. 12. Calculated maximum values of C_{pi} and C_p (C_d = 0.008) as functions of the turbine number of blades

stream are not univocally determined. It is difficult to determine the parameters b_V and m_V for a turbine with finite number of blades. However, the above presented results of numerical calculations lead to the following recommendations for the wind turbine designers:

- the design point of an axial wind turbine should be located at low advance coefficients,
- the optimum pitch of a wind turbine blades lies near the value P/D = 0.6,
- the computed effectiveness coefficient C_p of a turbine increases with the number of blades, but for real turbines operating in viscous fluid and suffering from flow deformations near the hub, which grow with increasing number of blades, the number of blades should not be too high.

CONCLUSION

Analyzing the above results it may be concluded that the models of ideal propulsor and ideal screw propeller correlate well with the experimental data. The efficiency of real propellers is always lower than that of the ideal ones and the effectiveness coefficient (defined as the ratio of real propeller efficiency to the efficiency of an ideal one) characterizes correctly the losses connected with fluid viscosity and with the finite number of real propeller blades.

The problem of turbines is significantly different, namely:

- there is no correlation between the experimental results and the results of calculations,
- the analogy between a turbine and an ideal fluid brake, for which the axial induced velocity component m_V is the basic parameter defining the performance, is a misunderstanding,
- the turbine performance is characterized by its torque: the model of an ideal turbine reduces the values of C_p as function of m_V even further than the model of an ideal brake, but as it was mentioned earlier the torque is not well correlated with m_V,
- when the results of model experiments are accepted as more trustworthy than calculations based on ideal models, the inadequacy of the Betz theorem for the determination of the limiting maximum value of the turbine effectiveness must be also accepted.

BIBLIOGRAPHY

1. Prandtl L., Betz A.: *Schraubenpropeller mit geringstem Energieverlust*, enthalten in "Vier Abhandlungen zur Hydrodynamik und Aerodynamik", Goettingen, Reprint 1927.
2. Chaja P., Góralczyk A., Koronowicz T.: *Experimental and Numerical Investigation of Small Axial Turbines*, TASK Quarterly vol. 14 No 3, 2011.
3. Koronowicz T.: *The Influence of the Cavitation Tunnel Walls on the Propeller Characteristics* (in Polish), Bulletin of IFFM No 356/1965.
4. Koronowicz T.: *The Theoretical Model of the Propeller Slipstream Based on the Concentrated Form of Vorticity with Cavitating Kernels and Hydrodynamic Characteristics of the System of Helicoidal Vortices in Bounded Fluid Domain* (in Polish), Scientific Papers of the IFFM No 58/956/1979.

CONTACT WITH THE AUTHORS

Tadeusz Koronowicz, Prof. (Emeritus),
The Szewalski Institute of Fluid Flow Machinery
Polish Academy of Sciences
Fiszera 14
80-952 Gdansk, POLAND
email: ttk@interecho.com

Jan A.Szantyr, Prof.,
Faculty of Mechanical Engineering
Gdansk University of Technology
Narutowicza 11/12
80-233 Gdansk, POLAND
email: jas@pg.gda.pl